

COMBINATORIAL CONDITIONS THAT IMPLY WORD-HYPERBOLICITY FOR 3-MANIFOLDS

MURRAY ELDER¹, JON MCCAMMOND¹, AND JOHN MEIER

ABSTRACT. Thurston conjectured that a closed triangulated 3-manifold in which every edge has degree 5 or 6, and no two edges of degree 5 lie in a common 2-cell, has word-hyperbolic fundamental group. We establish Thurston's conjecture by proving that such a manifold admits a piecewise Euclidean metric of non-positive curvature and the universal cover contains no isometrically embedded flat planes. The proof involves a mixture of computer computation and techniques from small cancellation theory.

1. INTRODUCTION

In this article we show that a class of closed triangulated 3-manifolds can be assigned a metric of non-positive curvature. In addition to proving a conjecture of Thurston, our main result illustrates the way in which the computer program developed by the first and second authors ([6]) can be used in conjunction with combinatorial methods to establish non-trivial results about 3-manifolds. The class of triangulations we consider are defined as follows.

Definition 1.1 (*5/6*-triangulations*). Let M be a closed triangulated 3-manifold and recall that the *degree* of an edge is the number of closed tetrahedra which contain it. If every edge in M has degree 5 or 6 then this is a *5/6-triangulation* of M . The triangulation is called a *5/6*-triangulation* if each 2-cell in M contains at most one edge of degree 5.

Thurston conjectured that every closed 3-manifold that admits a 5/6*-triangulation has word-hyperbolic fundamental group. We prove a slightly stronger version of this conjecture.

Theorem 1.2 (Main Theorem). *Every 5/6*-triangulation of a closed 3-manifold M admits a piecewise Euclidean metric of non-positive curvature, where the universal cover \widetilde{M} contains no isometrically embedded flat planes. As a consequence, $\pi_1(M)$ is word-hyperbolic.*

¹Partially supported under NSF grant DMS-0101506

Date: November 10, 2018.

2000 *Mathematics Subject Classification*. 20F06,57M50.

Key words and phrases. 3-manifolds, word-hyperbolic, non-positive curvature, CAT(0).

Such triangulations are not as special as they might appear. Cooper and Thurston show that every closed 3-manifold can be cellulated so that each 3-cell is a cube and each edge degree is 3, 4, or 5 [4]. Using similar techniques, Noel Brady and the last two authors show that every closed 3-manifold admits a triangulation where each edge degree is 4, 5, or 6 [2]. The dual concept — 5/6-triangulations where 2-cells contain at most one edge of degree 6 — is called a *foam* and is of interest in chemistry (see [9]).

Structure of the paper: In Sections 2 and 3 we use ideas resembling small cancellation theory to investigate the 2-sphere triangulations that arise as vertex links in 5/6*-triangulations of 3-manifolds. In Section 4 we review the general algorithm for determining curvature properties in 3-dimensional metric polyhedral complexes and establish an improved version of this algorithm that uses a lemma of Bowditch to greatly simplify the calculations. We describe the piecewise Euclidean metric we assign to a 5/6*-triangulation of a 3-manifold in Section 5, and in Section 6 we compare the computational results for this metric with the combinatorial restrictions proved in Section 3. Their mismatch enables us to establish our main result.

2. DIAGRAMS AND DUALS

In this section we recall some standard definitions and introduce soccer diagrams, which are closely associated with 5/6*-triangulations of 3-manifolds. For background on disc diagrams see [8].

Definition 2.1 (Disc diagram). A *disc diagram* D is a contractible combinatorial 2-complex together with a specific planar embedding $D \rightarrow \mathbb{R}^2$. If D is homeomorphic to a disc, D is *non-singular*, otherwise it is *singular*.

Definition 2.2 (Internal dual). Let D be a disc diagram in which all vertices of degree 2 lie on the boundary cycle of D . The *internal dual* of D is a subspace of D which consists of a 0-cell at the center of each 2-cell of D , a 1-cell passing through each internal 1-cell of D connecting the centers of the 2-cells on either side, and a 2-cell for each interior 0-cell v . See Figure 4 for an illustration. A similar definition can be given when D is a triangulation of a 2-sphere, which results in a *dual cellulation*.

The following lemma records the basic properties of internal duals. See Lemma 5.6 in [8] for a detailed proof.

Lemma 2.3 (Dual properties). *If D is a non-singular disc diagram and E is its internal dual, then E is a contractible, but possibly singular, disc diagram. Moreover, if R is a 2-cell in D and v is the corresponding 0-cell in E , then the number of components of $\partial R \cap \partial D$ equals the number of components of the link of v .*

Terminology 2.4 (Paths, loops, vertex degrees). Throughout this paper, *paths* and *loops* in a cell complex are edge paths and loops. The *degree* of a vertex v is the number of edges incident with v .

Definition 2.5 (Sphere triangulation). If M is a $5/6^*$ -triangulation of a 3-manifold, the link of a vertex in M is a triangulation of a 2-sphere in which each vertex has degree 5 or 6 and no two vertices of degree 5 are connected by an edge. A triangulated 2-sphere with both of these properties is called a $5/6^*$ -triangulation of a 2-sphere.

Definition 2.6 (Soccer diagram). Let D be a $5/6^*$ -triangulation of a 2-sphere and let E denote its dual cellulation. Since vertices in D have degree 5 or 6, the dual consists of pentagons and hexagons; since D is a triangulation, every vertex in E has degree 3; and since no two vertices degree 5 in D are connected by an edge, no two pentagons in E share a common side. The cell structure E is called a *soccer tiling* of the 2-sphere since the standard tiling of a soccer ball is a simple example with all of these properties. A subcomplex of a soccer tiling of a 2-sphere, which is homeomorphic to a disc, is called a *soccer diagram*. Notice that the embedding of a soccer diagram into the 2-sphere determines a natural planar embedding as well. Thus soccer diagrams are disc diagrams and the definition further implies that they are non-singular.

Definition 2.7 (Left/right turn). Let P be an immersed directed path in a soccer tiling. If the sphere is oriented then there is a well-defined notion of a *left/right turn* (the 2-cells are thought of as convex and approximately regular). These are the only possibilities since every vertex has degree 3. The *turn pattern* for P is the sequence of left and right turns. For soccer diagrams we define a turn pattern by traversing the boundary cycle counterclockwise in the induced orientation. (Since every vertex in ∂D has a connected link and is of degree 2 or 3, the boundary vertices of degree 2 correspond to left turns and those of degree 3 to right turns.) Finally, let n_l and n_r denote the total number of left and right turns, respectively. The difference $n_l - n_r$ is the *combinatorial turning angle*.

The combinatorial turning angle is directly related to the number of pentagons D contains.

Lemma 2.8 (Turns and pentagons). *If D is a soccer tiling of a 2-sphere then D contains exactly twelve pentagons. Moreover, if D is a soccer diagram containing exactly p pentagons, the combinatorial turning angle is $6 - p$. Hence $p \leq 6$ implies $n_l \geq n_r$.*

Proof. We sketch a proof using the Combinatorial Gauss-Bonnet Theorem: For any angle assignment, the sum of the vertex curvatures plus the sum of the face curvatures is always 2π times the Euler characteristic. (See for example [8, Section 4].) If we assign an angle of $2\pi/3$ to each corner of each 2-cell, the hexagons have curvature 0, the pentagons have curvature $\pi/3$, the internal vertices have curvature 0, the vertices located at left turns have curvature $\pi/3$ and the vertices located at right turns have curvature $-\pi/3$. Thus $2\pi \cdot 2 = (\pi/3) \cdot p$ for a soccer tiling, and $2\pi \cdot 1 = (\pi/3) \cdot (p + n_l - n_r)$ for a soccer diagram. Dividing by $\pi/3$ and rearranging yields the results. \square

Remark 2.9 (Limiting pentagons). If P is a simple closed loop embedded in a soccer tiling D , then it bounds two soccer diagrams D_1 and D_2 whose intersection is P and whose union is D . Since D contains only twelve pentagons, P always bounds some soccer diagram with at most six pentagons.

Definition 2.10 (Exposed path). If D is a soccer diagram whose turn pattern contains $i - 1$ consecutive left turns, then D contains a 2-cell R such that ∂R and ∂D share a path of length i . We call this an *exposed path of length i* and R is the 2-cell which is *exposed*.

Corollary 2.11 (Alternating turns). *If D is a soccer diagram with at most six pentagons, then either D contains an exposed path of length 3, or the turn pattern is $(rl)^i$ for some i and D contains exactly six pentagons.*

Proof. By Lemma 2.8, $n_l \geq n_r$. If $n_l > n_r$, two left turns must be adjacent, creating an exposed path of length 3. On the other hand, if $n_l = n_r$, then the only way to avoid adjacent left turns is for the left and right turns to alternate. This, in turn, implies exactly six pentagons by Lemma 2.8. \square

3. SMALL DIAGRAMS

In this section we prove a key technical result about soccer diagrams with short boundary cycles, Theorem 3.10. We begin by examining two processes by which soccer diagrams can be decomposed into smaller soccer diagrams: cut paths and double duals.

Definition 3.1 (Cut path). A soccer diagram D has a *cut path* if there are two soccer diagrams D_1, D_2 such that $D = D_1 \cup D_2$ and $D_1 \cap D_2$ is a simple path P . See Figure 1. If D has at least one cut path, then it has a cut path of minimum length; in Figure 1 this minimum is 2.

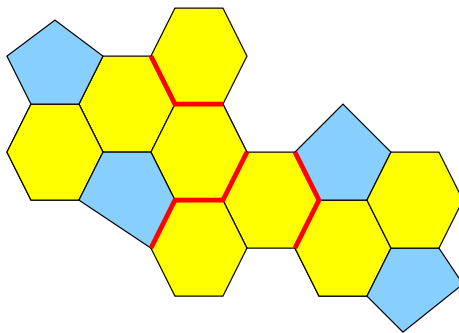


FIGURE 1. A soccer diagram with several cut paths marked by thick lines.

Lemma 3.2 (Cut paths exist). *If D is a soccer diagram with at least two 2-cells then D has a cut path. If, in addition, D has at most six pentagons then D has a cut path of length at most 4.*

Proof. Choose a 2-cell R such that an edge of ∂R is contained in ∂D . Since D has more than one 2-cell, ∂D and ∂R are distinct and there exists a subpath of ∂R which starts and ends in ∂D and otherwise is contained in the interior of D . This is a cut path whose length is at most 5. If the shortest cut path has length 5 then every 2-cell containing a edge of ∂D must be a hexagon with exactly one edge in ∂D , but this would imply ∂D contains only right turns, contradicting Lemma 2.8. \square

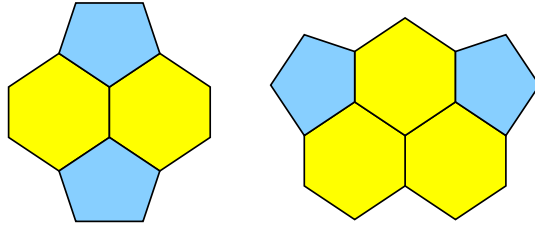


FIGURE 2. Soccer diagrams with few 2-cells and no exposed path of length 4.

Lemma 3.3 (Small diagrams). *If D is a soccer diagram with at most five 2-cells, then D contains a cut path of length at most 2. If in addition, D does not contain an exposed path of length at least 4, then D is one of the two disc diagrams shown in Figure 2.*

Proof. Rather than analyze D directly, it is easier to analyze its internal dual E . By Lemma 2.3, E is a (possibly singular) disc diagram with at most 5 vertices and all of the possibilities for E are shown in Figure 3. Notice that every possibility for E contains either a vertex of degree 1, or a triangle with a vertex of degree 2, and these lead to cut paths of length 1 and 2 in D .

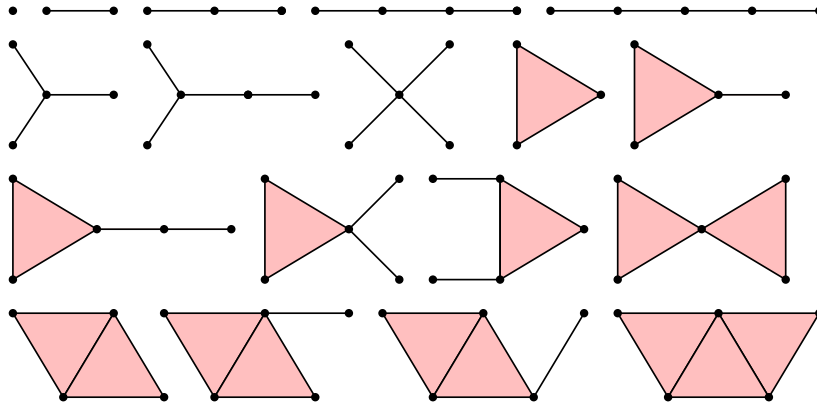


FIGURE 3. Simplicial disc diagrams with at most 5 vertices.

To see the second assertion, notice that a vertex in E of degree 1 corresponds to a 2-cell R in D such that only one edge of ∂R lies in the interior of D , hence the remaining edges form an exposed path of length ≥ 4 . Similarly, if E contains a triangle in which two of its vertices have degree 2, then these vertices correspond to 2-cells in D , at least one of which must be a hexagon. This hexagon also creates an exposed path of length 4 in D .

There are only two diagrams in Figure 3 that contain neither vertices of degree 1 nor triangles with two vertices of degree 2 (i.e. the diagrams in the lower left-hand corner and lower right-hand corner). In both cases, the vertices in E of degree 2 must correspond to pentagons in D in order to avoid exposed paths of length 4, and the remaining vertices must correspond to hexagons since they share sides with the pentagons. Thus there are exactly two possibilities for D , and these are the ones shown in Figure 2. \square

The remainder of the section is devoted to showing that soccer diagrams with more than five 2-cells and at most six pentagons have long boundary cycles (Lemma 3.9). The proof of Lemma 3.9 proceeds by induction and the following lemma provides the basis step.

Lemma 3.4 (Minimum length). *Let D be a soccer diagram with k 2-cells and at most six pentagons. For $k = 1, 2, 3, 4, 5, 6$, the minimal length of ∂D is 5, 9, 11, 12, 14, 15, respectively.*

Proof. In Figure 4 we exhibit soccer diagrams that realize these values, so the only question is whether there are diagrams with smaller boundary cycles. Let E be the internal dual of D . If $k \leq 5$, then E is one of the diagrams listed in Figure 3 and it is straightforward to enumerate all of the possibilities for D given a specific E and to calculate that the diagrams shown in Figure 4 have minimal length boundary cycles for these values of k .

Now suppose $k = 6$. If E contains either a vertex of degree 1 or a triangle with a vertex of degree 2, then D contains a 2-cell R which is separated from the rest of D by a cut path of length at most 2. Removing R and the exposed portion of ∂R from D creates a new soccer diagram D' with exactly five 2-cells, and $|\partial D'| \geq 14$. Since R is either a pentagon or a hexagon, reattaching R to D' shows that $|\partial D| \geq 15$. The only six-vertex simplicial disc diagram E that does not contain a vertex of degree 1 or a triangle with a vertex of degree 2 is the one whose 1-skeleton is superimposed on the soccer diagram in the lower left-hand corner of Figure 4. For this E , the internal vertex must correspond to a pentagon thereby forcing all of the other vertices to correspond to hexagons. In other words, the soccer diagram shown is the only soccer diagram whose internal dual is E , and the inequality follows. \square

The second process we investigate is the process of taking double duals.

Remark 3.5 (Double duals). Let D be a soccer diagram and let D' be the internal dual of the internal dual of D (i.e. its *double dual*). While it is true that D' is a subcomplex of D (it is essentially D minus the open star of its boundary), it is not automatically true that D' itself is a soccer diagram,

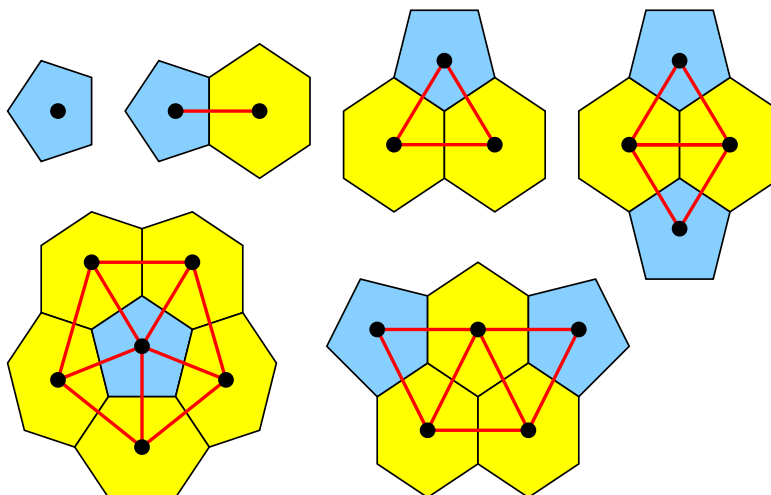


FIGURE 4. Soccer diagrams with k 2-cells and minimal boundary lengths for k equals 1 up to 6. In each case, the 1-skeleton of its internal dual has been superimposed.

since D' need not be connected and it might be singular. These situations are illustrated in Figures 5 and 6.

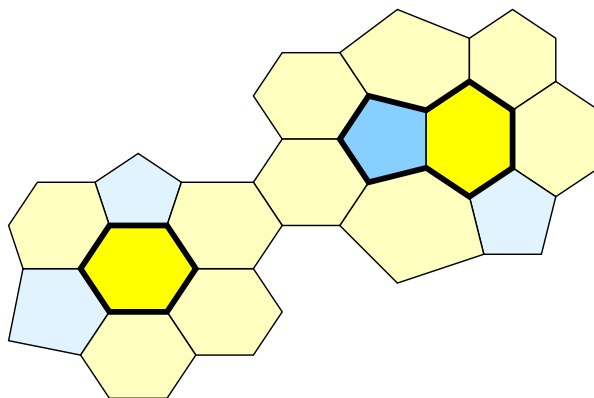


FIGURE 5. A soccer diagram whose double dual is not a soccer diagram because it is disconnected.

Lemma 3.6 (Double duals). *Let D be a soccer diagram and let D' be its double dual. If D' is disconnected, then D contains a cut path of length at most 2. If D' is connected, but singular, then the turn pattern for D contains either two consecutive left turns or two consecutive right turns.*

Proof. Let E denote the dual of D . If D' is disconnected, there are triangles in E that cannot be connected by a sequence of triangles so that successive

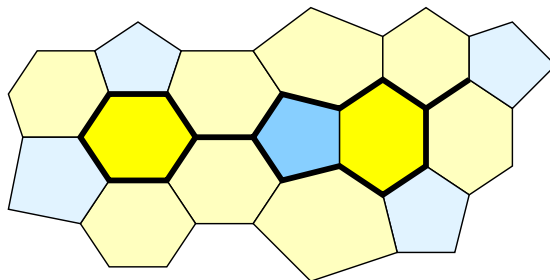


FIGURE 6. A soccer diagram whose double dual is not a soccer diagram because it is nonsingular.

triangles share a common side. Since E itself is connected (Lemma 2.3), this implies that E contains a vertex v whose removal disconnects E and separates one triangle from another. Let R be the 2-cell in D corresponding to v . By Lemma 2.3, $\partial R \cap \partial D$ is disconnected. Since vertices have degree at most three, the components of $\partial R \cap \partial D$ are non-trivial paths. Thus a portion of ∂R creates a cut path of length at most 2.

If D' is connected but singular, at least one of two situations must occur: D' contains a vertex of degree 1 (a *spur*) and/or a vertex whose removal disconnects D' (a *cut vertex*). Both possibilities are illustrated in Figure 6.

If v is a spur, then there are two edges of $D \setminus D'$ incident with v that form a cut path separating the 2-cell R of D containing these two edges from the rest of the diagram. Since $|\partial R| \geq 5$, this creates an exposed path of length 3 and two consecutive left turns in the turn pattern of D .

Vertices in D' have degree at most three, and cut vertices have disconnected links, so cut vertices are always incident with an edge that is not in the boundary of a 2-cell of D' . By following a tree of possibilities, we can always find a spur in D' or a vertex v that has a disconnected link and lies in the boundary of a 2-cell of D' . There are two 2-cells in $D \setminus D'$ that contain v , and these 2-cells must each have 2 edges incident with 2-cells in the ring $D \setminus D'$. Of the two 2-cells of $D \setminus D'$ that contain v , at least one has $|\partial R \cap D'| \geq 3$. Because vertices have degree at most three, and five edges of R are already accounted for, R must be a hexagon that shares only one edge with ∂D and the vertices of this edge yield two consecutive right turns. \square

Corollary 3.7. *If D is a soccer diagram whose turn pattern is $(rl)^i$ and whose shortest cut path has length at least 3, then its double dual D' is a soccer diagram. Moreover, $|\partial D'| = 2i - p$ where p is the number of pentagons that contain an edge in ∂D .*

Proof. By Lemma 3.6, D' must be both connected and nonsingular. Thus it is homeomorphic to a disc and consequently a soccer diagram. To prove the second assertion notice that there are exactly i 2-cells in the ring of 2-cells removed from D to create D' . Moreover, each of these 2-cells has two of its edges in ∂D and another two edges are shared with neighboring 2-cells in

the ring. Thus each hexagon in the ring contributes two edges to $\partial D'$ and each pentagon contributes one. \square

Corollary 3.8 (Removing rings). *Let D be a soccer diagram with at most six pentagons. If the length of the shortest cut path is 4 then the double dual of D is a soccer diagram D' containing exactly six pentagons and $|\partial D| = |\partial D'|$.*

Proof. If D contains an exposed path of length 3 then there would be a cut path of length less than 4. Thus exposed paths of length 3 cannot exist and by Corollary 2.11, the turn pattern for D is $(rl)^i$ for some i , and D contains exactly six pentagons. As a consequence of the left/right alternation, every 2-cell sharing an edge with ∂D actually shares two consecutive edges. Thus pentagons sharing an edge with ∂D lead to cut paths of length less than 4 and all of 2-cells touching ∂D are hexagons. The result now follows immediately from Corollary 3.7. \square

Our key technical result about soccer diagrams is that large diagrams have long boundary cycles.

Lemma 3.9 (Large implies long). *If D is a soccer diagram with at least six 2-cells and at most six pentagons, then $|\partial D| \geq 15$.*

Proof. We induct on the number of 2-cells. By Lemma 3.4 the statement is true for $k = 6$, so suppose it is true for some $k \geq 6$ and let D be a soccer diagram with exactly $(k + 1)$ 2-cells. By Lemma 3.2, D contains a cut path of length at most 4. Let P be a cut path of minimal length and consider the number of 2-cells in D_1 and D_2 . Without loss of generality assume that D_2 has at least as many 2-cells as D_1 .

Case 1: If D_1 has at least three 2-cells, then D_2 has at least four 2-cells and by Lemma 3.4, $|\partial D_1| + |\partial D_2| \geq 23$. Since $|P| \leq 4$ and $|\partial D| = |\partial D_1| + |\partial D_2| - 2|P|$, we conclude $|\partial D| \geq 15$.

Case 2: If D_1 has two 2-cells, then D_2 has at least five, and by Lemma 3.4, $|\partial D_1| + |\partial D_2| \geq 23$ and as in Case 1, $|\partial D| \geq 15$.

Case 3: If D_1 has one 2-cell, then D_2 has at least six, and by Lemma 3.4, $|\partial D_1| + |\partial D_2| \geq 20$. If $|P| \leq 2$, then $|\partial D| \geq 16$. If $|P| = 4$, then by Corollary 3.8 ∂D has the same length as the boundary of its double dual D' which is itself a soccer diagram with at least six 2-cells. By induction $|\partial D'| \geq 15$, and the inequality holds. Thus we may assume $|P| = 3$. If $|\partial D_1| > 5$ or $|\partial D_2| > 15$, then $|\partial D| \geq 15$, so we may also assume D_1 is a pentagon and $|\partial D_2| = 15$. This would produce a soccer diagram D with $|\partial D| = 14$. To summarize, the only way for the induction to fail is if there exists a soccer diagram D with $|\partial D| = 14$ whose shortest cut path has length 3 and separates a pentagon from the rest of D .

If the boundary of this hypothetical diagram contains an exposed path of length 3, then the 2-cell it exposes is a hexagon, since otherwise there is a cut path of length 2. Removing this hexagon does not change the length of the boundary, and it creates a diagram D' with $|\partial D'| \geq 15$ by induction.

Thus exposed paths of length 3 do not occur. By Corollary 2.11 the turn pattern is $(rl)^i$, D contains exactly six pentagons, and $i = 7$ since $|\partial D| = 14$.

Let D' denote the double dual of D . By Lemma 3.6, D' is a soccer diagram with $|\partial D'| \leq 13$ since D contains at least one pentagon which shares an edge with ∂D . By the induction hypothesis D' has at most five 2-cells and by Lemma 3.4 it actually has at most four. On the other hand, the ring removed from D to create D' only contained seven 2-cells and at most three of these could be pentagons since the pentagons must be non-adjacent. Thus D' contains at least three pentagons. Finally, the only soccer diagram with at most four 2-cells and at least three pentagons is a hexagon with three pentagons attached to alternate edges. Since it is impossible to reconstruct D by attaching a ring containing a pentagon to this D' , we conclude that D cannot exist. \square

Our key result about soccer diagrams follows immediately from Lemmas 3.3 and 3.9.

Theorem 3.10. *If D is a soccer diagram with $|\partial D| \leq 14$, at most six pentagons, and no exposed path of length 4, then D is one of the disc diagrams shown in Figure 2.*

4. ALGORITHM

In this section we review and improve (via a result of Bowditch) the algorithm for testing the curvature properties of finite piecewise Euclidean 3-complexes given in [6]. For background on non-positive curvature and piecewise Euclidean complexes, see [3].

A geodesic in a geodesic metric space is *short* if its length is strictly less than 2π and *very short* if strictly less than π . The original algorithm is based on the standard link condition for piecewise Euclidean complexes.

Theorem 4.1 (Link Condition). *A piecewise Euclidean complex is non-positively curved if and only if the link of each cell has no short closed geodesic.*

Thus deciding whether or not a piecewise Euclidean complex is non-positively curved depends on checking piecewise spherical complexes for short geodesics. Geodesics of this type determine complexes we call “circular galleries”. Rather than give a full technical definition of a circular gallery, we give a rough definition and an example. The reader is referred to [5] and [6] for precise details.

Definition 4.2 (Galleries). If γ is a geodesic in a piecewise spherical complex then the ordered list of closed simplices through which γ passes encodes a *linear gallery determined by γ* . If γ is a closed geodesic, this list is given a cyclic rather than a linear ordering and the result is called the *circular gallery determined by γ* . Linear and circular galleries can also be determined by paths which are merely close to geodesics.

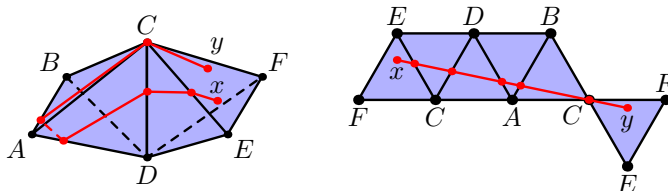


FIGURE 7. The 2-complex and linear gallery described in Example 4.3.

Example 4.3. Let K be the 2-dimensional piecewise spherical complex formed by attaching the boundaries of two regular spherical tetrahedra along a 1-cell. The complex K is shown on the left of Figure 7 (where the spherical nature of the 2-cells has been left to the reader's imagination). Let γ be the geodesic shown, which starts at x travels across the front of K , around the back, over the top, and ends at y . The linear gallery determined by γ is shown on the right.

In [5] the first two authors prove that given any finite piecewise Euclidean complex there exists an algorithm to decide if it is non-positively curved. In dimension 3 a second, more geometric algorithm is available, which has been implemented as a computer program `cat.g` written in GAP [7].

The current version of the program is designed to be used with Euclidean tetrahedra whose edge lengths are square-roots of rationals. This restriction enables the use of exact arithmetic since all of the calculations can be carried out in an algebraic number field. The program examines the circular galleries that can occur in the the link of a vertex. The links of other cells in 3-complexes are easy to check without a computer. There are four types of 2-dimensional piecewise spherical circular galleries which need to be considered. If the geodesic passes through a vertex, the gallery is made up of vertex-to-vertex segments called *beads*, which join together to form a *necklace*. If it does not pass through a vertex, the gallery it determines is either a disc, an annulus, or a Möbius band. Since disc galleries containing short closed geodesics can only exist in complexes in which the edge links contain short closed geodesics, these need not be considered.

The number of spherical triangles in a circular gallery containing a short closed geodesic can be bounded ahead of time using only the list of Euclidean tetrahedra. Roughly speaking the computer program proceeds by enumerating every feasible annular or Möbius gallery and every bead up to this bound, cuts them open and develops them onto the 2-sphere calculating explicit coordinates as it goes. Then it uses elementary linear algebra to check each for the existence of a short closed geodesic. Details on the algorithm can be found in [6]; the program is available from the authors' web-pages. The cutting open and developing process is illustrated in Figure 8.

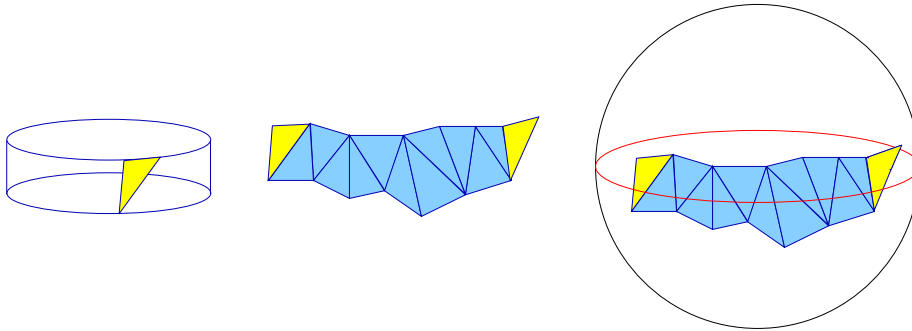


FIGURE 8. An annular gallery, cut open and developed.

In the remainder of this section we show how the computations described in [6] can be simplified using a result by Brian Bowditch [1]. Throughout the remainder of the section let S denote a locally CAT(1) space.

Definition 4.4 (Unshrinkable). A closed geodesic γ in S is *shrinkable* if there is a homotopy starting at γ such that the length of the closed curve is non-increasing as a function of time and ends at a curve whose length is strictly less than its initial length. Notice that only the initial curve is required to be a geodesic, so the equator on a standard metric 2-sphere is shrinkable. A closed geodesic that is not shrinkable is *unshrinkable*. Even if a closed geodesic is not shrinkable, there may exist a homotopy such that the length of the closed curve is unchanging as a function of time. In this case we say that the curves at either end are *equivalent*.

In this terminology, Bowditch's result can be restated as follows:

Lemma 4.5 (Unshrinkable). *If S is a locally CAT(1) space that is not globally CAT(1), then the length of the shortest closed geodesic is the same as the length of the shortest unshrinkable closed geodesic.*

This leads immediately to the following refinement of the link condition.

Corollary 4.6 (Link condition). *If S is a locally CAT(1) space that does not contain a short unshrinkable closed geodesic, then S is globally CAT(1). As a consequence, a piecewise Euclidean complex is non-positively curved if and only if the link of each cell has no short unshrinkable closed geodesic.*

As the next three lemmas show, restricting to unshrinkable geodesics reduces the number of galleries one needs to inspect.

Lemma 4.7 (Shrinking annular galleries). *Let γ be a closed geodesic in a 2-dimensional locally CAT(1) piecewise spherical complex S . If γ determines an annular gallery \mathcal{G} , then γ is shrinkable.*

Proof. When \mathcal{G} is cut open and developed, γ is sent to part of a great circle on the 2-sphere. The homotopy which pushes this path through different lines

of latitude shrinks its length and corresponds in \mathcal{G} to a shorter closed path. Thus γ is shrinkable. See the left-hand side of Figure 9 for an illustration. \square

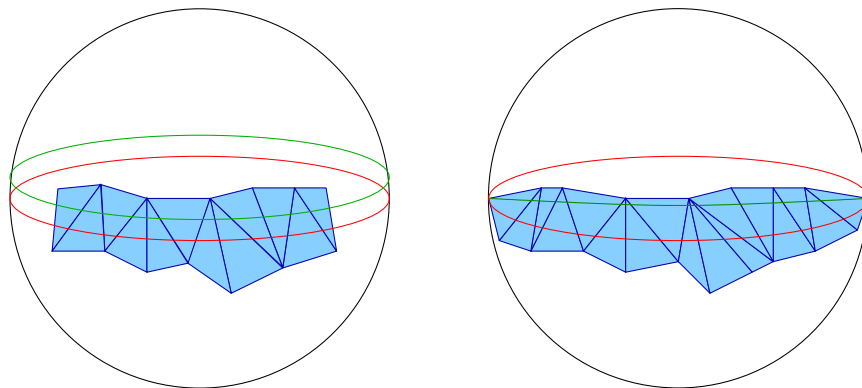


FIGURE 9. Two examples of how geodesics can be tipped

Lemma 4.8 (Shrinking Möbius galleries). *Let γ be a closed geodesic in a 2-dimensional locally CAT(1) piecewise spherical complex S . If γ determines a Möbius gallery and the length of γ is at least π , then γ is shrinkable.*

Proof. When \mathcal{G} is cut open and developed, γ is sent to path γ' in a great circle on the 2-sphere of length at least π . Let u and v be points in γ' that are antipodal. The portion of γ' between u and v can be homotoped (in a non-length-changing way) to another geodesic length π connecting them without having the image leave the image of the cut open Möbius gallery. This new path is not locally geodesic at u or v and can be shortened at either end to produce a strictly shorter path. Thus γ is shrinkable. See the right-hand side of Figure 9 for an illustration. \square

Lemma 4.9 (Tipping Beads). *Let γ be a closed geodesic in a 2-dimensional locally CAT(1) piecewise spherical complex S . If γ determines a necklace gallery \mathcal{G} such that a single bead contains a portion of γ of length strictly more than π , then γ is shrinkable. Moreover, if γ determines a necklace gallery \mathcal{G} that contains a single bead containing a portion of γ of length exactly π , then γ is equivalent to a path γ' which determines a necklace gallery in which all beads contain strictly less than π of γ' .*

Proof. If there is a bead containing more than π of γ , then we can pick u and v in the interior of the bead which are connected by a portion of γ of length exactly π . The rest of the proof mimics the proof of Lemma 4.8. If there is a bead containing a portion of γ of length exactly π , then we pick the vertices at either end through which γ passes as our u and v and proceed to tip the portion of γ between them. Because the link of u may have excess curvature, we do not know that γ can be locally shortened after γ has been tipped. On the other hand, we can continue tipping the portion of γ between u and v

until the path hits the boundary cycle of the bead. Because this boundary cycle is a piecewise geodesic path, the portion of its boundary included in the tipped path must include a new vertex of \mathcal{G} . Since γ is assumed to be short, there is only one bead of length π , and in this equivalent path this one long bead has been broken up into at least two shorter ones. \square

The original program searched for all annular and Möbius galleries that contain short closed geodesics and all beads which contain geodesics of length less than 2π , which are then strung together to form necklaces. By the last three lemmas we do not need to search for annular galleries at all, or for the longer types of beads and Möbius galleries. To appreciate the magnitude of this simplification see Remark 5.7.

5. METRIC AND OUTPUT

We begin this section by defining the shapes used to give $5/6^*$ -triangulated 3-manifolds piecewise Euclidean structures.

Definition 5.1 (The metric). Let M be a $5/6^*$ -triangulated, closed 3-manifold. We make M a *metric $5/6^*$ -triangulated 3-manifold* by assigning a length of $\sqrt{3}$ to each edge of degree 6, a length of 2 to each edge of degree 5, and metrics of the unique Euclidean simplices whose edge lengths match those assigned to their 1-skeletons to the triangles and tetrahedra.

Definition 5.2 (The tetrahedra). The fact that edges of degree 5 cannot belong to the same 2-cell means that there are only three equivalence classes of metric tetrahedra in M : those with 0, 1 or 2 edges of degree 5. See Figure 10. Notice that the first tetrahedron is regular and the third one is a Coxeter shape with dihedral angles $\pi/2$ and $\pi/3$ around the edges of degree 5 and 6, respectively. We refer to these three metric tetrahedra as *regular*, *mixed* and *Coxeter* tetrahedra.

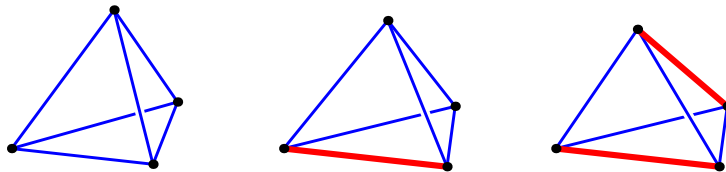


FIGURE 10. The three types of tetrahedra (regular, mixed, and Coxeter) in a $5/6^*$ -triangulation. The thin edges have length $\sqrt{3}$ and the thick edges have length 2.

Straightforward computations show:

Lemma 5.3 (Dihedral angles). *Let M be a closed 3-manifold with a metric $5/6^*$ -triangulation and let e be an edge in a tetrahedra T in M . If e has degree 5, then the dihedral angle in T at e is more than $2\pi/5$ and at most $\pi/2$. If e has degree 6, then the dihedral angle in T at e is at least $\pi/3$, strictly*

less than $\pi/2$, and equal to $\pi/3$ only if T is Coxeter. As a consequence, the links of edges in M are metric circles of length at least 2π and exactly 2π if and only if e has degree 6 and is surrounded by six Coxeter tetrahedra.

The software `cat.g` returns a list of 4 trivial beads, 71 non-trivial beads and 144 Möbius galleries, for these three tetrahedra. Because we are interested in triangulated 3-manifolds, and Möbius strips cannot be immersed into 2-spheres, the Möbius strips in the output can be safely ignored.

Definition 5.4 (Bead types). Combinatorially all 75 metric beads of length less than π in the output look like the one of the three non-metric beads shown in Figure 11. The differences come from the metrics. Specifically there are 4 different metric edges, 26 metric beads consisting of two triangles, and 45 metric beads consisting of four triangles. We refer to these underlying combinatorial structures as beads of *type A*, *type B* and *type C* respectively. In each case, the geodesic contained in the bead starts at the leftmost vertex and ends at the rightmost vertex.

Similarly, the *type of a necklace*, refers to its underlying combinatorial structure, rather than its metric. A necklace containing at least one non-trivial bead is called a *thick necklace* while those consisting solely of trivial beads are called *thin necklaces*.

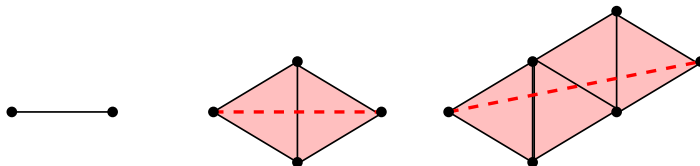


FIGURE 11. The three types of beads.

The following estimates on the lengths of geodesics in each of the three bead types immediately implies Corollary 5.6.

Lemma 5.5 (Lower bounds). *The length of a geodesic in a bead of type A, B or C is bounded below by $.304\pi$, $.5\pi$, and $.832\pi$, respectively.*

Corollary 5.6 (Necklaces). *There are 28 types of necklaces consisting of short beads that might contain a closed geodesic of length less than 2π . These 28 possibilities are $A, A^2, A^3, A^4, A^5, A^6, B, AB, A^2B, A^3B, A^4B, B^2, AB^2, A^2B^2, ABAB, A^3B^2, A^2BAB, C, AC, A^2C, A^3C, BC, ABC, A^2BC, ABAC, B^2C, C^2$, and AC^2 .*

Remark 5.7 (Speed). The entire computation took less than one hour to complete on a 850MHz PC running GAP under Linux. It tested approximately 110 thousand galleries and yielded the 75 beads described above. As an indication of the benefits of the simplification described in Section 4, we note that an earlier computer search — using the original algorithm — took

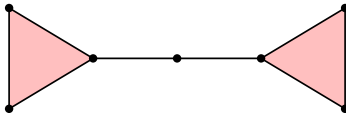


FIGURE 12. A barbell with 3 cut vertices.

more than 2 months to complete, tested approximately 300 million galleries and yielded $\simeq 12000$ beads. Moreover, instead of the three combinatorial types shown in Figure 11, there were more than 100 combinatorial types. In other words, the restriction to unshrinkable geodesics not only improved the length of the computation, it also greatly simplified the output.

6. MAIN RESULT

Throughout this section let M be a metric $5/6^*$ -triangulation of a 3-manifold, let S be the link of a 0-cell in M , and let γ be a closed geodesic contained in S which determines a necklace gallery \mathcal{G} consisting of short beads.

Definition 6.1 (Barbells). Let \mathcal{G} be a thick necklace gallery. The linear gallery consisting of a (possibly empty) sequence of trivial beads with a single triangle on either end is called a *barbell*. See Figure 12. Notice that a barbell containing $i - 1$ trivial beads contains exactly i cut vertices. Also note that the transition between two non-trivial beads leads to a barbell consisting of two triangles joined at a vertex.

Definition 6.2 (Good perturbations). If γ is perturbed slightly so that it avoids all of the vertices in S , then the circular gallery determined by the new path is an annular gallery. In order to maintain control over the combinatorial properties of the annular gallery which results, we define a *good perturbation* of γ as follows. If \mathcal{G} is a thin necklace, then γ' is the boundary curve of an ϵ -neighborhood of γ in S that passes through the minimum number of triangles. If both boundary curves pass through the same number of triangles, both boundary curves are good perturbations. If \mathcal{G} is a thick necklace, then define γ' one barbell at a time. In each barbell we consistently push the path γ' to the left of all the cut vertices or to the right of all the cut vertices, whichever minimizes the number of triangles through which it passes. See Example 6.3.

Example 6.3. Figure 13 shows a barbell in which the good perturbation lies above the three cut vertices. Since we are only interested in the gallery determined by the perturbed path (and not the path itself), the jagged line connecting the centers of the triangles is a perfectly good representative of the perturbed path.

We need two technical lemmas about the paths determined by good perturbations; one for thin necklaces and one for thick necklaces.

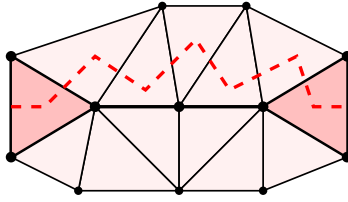


FIGURE 13. A barbell, its neighborhood and a perturbed geodesic.

Lemma 6.4 (Thin necklaces). *Let γ be a geodesic of length at most 2π which determines a thin necklace, let γ' be a good perturbation of γ and let P be the closed immersed path that is the internal dual of the annular gallery determined by γ' . If c is the absolute value of the combinatorial turning angle for P , then $|P| + c \leq 12$. Moreover, the turn pattern for P does not contain three consecutive left turns or three consecutive right turns.*

Proof. Since \mathcal{G} is thin it has type A^i for some i and by Lemma 5.5, $i \leq 6$. Notice that i is also the number of vertices in γ . For each vertex v in γ , the two boundary curves of an ϵ -neighborhood of γ pass through five or six corners of triangles. The triangles on either side of the trivial beads of γ are double counted in the sense that the boundary curves traverse two corners of these triangles in a row before moving on to a new triangle. They cannot traverse three corners in a row since this would require γ to traverse two sides of the triangle consecutively, and this is prohibited by the size of the dihedral angles (Lemma 5.3) and the fact that γ is a local geodesic. Thus the two paths together determine annular galleries that contain at most $4i$ triangles combined, and one annular gallery has at most $2i$ triangles.

Without loss of generality assume that the good perturbation is the one to the left of γ as γ is traversed. Let R be a triangle that contains a portion of γ' and notice that R corresponds to a vertex in P corresponding to a left turn if and only if ∂R contains an edge of γ . This implies that the turn pattern for P contains exactly i left turns and that $|P| + c = (n_l + n_r) + (n_l - n_r) = 2n_l = 2i \leq 12$.

Suppose P contains three consecutive right turns. The three triangles corresponding to these turns, plus the triangle immediately before and after (as traced out by γ'), all contain a common vertex v in their boundaries. Since v has degree at most 6, the path γ would have to make a sharp turn at v and γ would not be a local geodesic. If P contains three consecutive left turns, then there are three consecutive edges in γ (with separating vertices u and v) such that all three triangles to the left of these edges contain a common apex. In order for γ to be a local geodesic at u and v , by Lemma 5.3 both vertices would need to have degree 5, which is forbidden. \square

Lemma 6.5 (Thick necklaces). *Let γ be a short unshrinkable geodesic which determines a thick necklace consisting of short beads, let γ' be a good perturbation of γ , and let P be the closed immersed path that is the internal dual of*

the annular gallery determined by γ' . If c is the absolute value of the combinatorial turning angle for P , then $|P| + c \leq 14$. Moreover, the turn pattern for P does not contain three consecutive left turns or three consecutive right turns.

Proof. The proof is similar to Lemma 6.4, but it proceeds one barbell at a time. Consider a barbell in \mathcal{G} with i cut vertices. For each cut vertex v in the barbell, the two possible perturbations of γ pass through five or six corners of triangles. As before the triangles on either side of the trivial beads are double counted in the sense that the boundary curves traverse two corners of these triangles in a row before moving on to a new triangle. They cannot traverse three corners in a row since this would require γ to traverse two sides of the triangle consecutively, which is prohibited by the size of the dihedral angles (Lemma 5.3) and the fact that γ is a local geodesic. Since the triangles at either end already existed, the two possible perturbations pass through at most $6i - 2(i - 1) - 2 = 4i$ new triangles. In particular, one of them passes through at most $2i$ new triangles.

Without loss of generality assume that the good perturbation is the one to the left of the portion of γ in this barbell as γ is traversed. Let R be a triangle which is traversed by this portion of γ' and notice that R corresponds to a vertex in P which is a left turn if and only if ∂R contains a trivial bead of γ or R is one of the original two triangles in the barbell. This implies that this portion of the turn pattern for P contains exactly i left turns. As above, the number of vertices in this portion of P plus the absolute value of the combinatorial turning angle for this portion is twice the number of left turns for this portion, which is $2i$. Finally, notice that the only portions of P that are not contained in some barbell are the portions corresponding to the two interior triangles in a bead of type C . Since these two triangles become vertices in P which turn in opposite directions, they contribute to the length of P but not to c . It is now routine to calculate that 14 is an upper bound for $|P| + c$ for each of the 22 thick cases listed in Corollary 5.6. Finally, the arguments that P has no three consecutive left [right] turns is identical to the one given above and is omitted. \square

It is now relatively easy to show that the paths that good perturbations determine are in fact simple.

Lemma 6.6 (Simple). *Let γ be either a geodesic of length at most 2π which determines a thin necklace or a short geodesic which determines a thick necklace consisting of short beads. If P is the closed immersed path which is the internal dual of the annular gallery determined by a good perturbation of γ , then P is a simple closed path.*

Proof. Suppose P is not embedded and let Q be a closed subpath of P of minimal length. Since $|P| \leq 14$ by Lemma 6.4 and Lemma 6.5, $|Q| \leq 7$. Since Q itself is embedded it divides the soccer tiling into two soccer diagrams D_1 and D_2 , one of which, say D_1 , has fewer than six pentagons.

By Lemma 3.4, D_1 consists of a single 2-cell and thus P contains at least four consecutive left [right] turns, contradicting Lemma 6.4 or Lemma 6.5. \square

We can now show that our hypothetical short closed unshrinkable geodesic γ does not exist.

Lemma 6.7 (Vertex links). *If S is the link of a vertex in a metric $5/6^*$ -triangulated, closed 3-manifold, then it does not contain any short closed unshrinkable geodesics. In addition, S does not contain any closed geodesics of length 2π in its 1-skeleton.*

Proof. If S contains a short closed unshrinkable geodesic, then by Lemma 4.9 it also contains a short closed unshrinkable geodesic which determines a necklace consisting of short beads. Let γ be either a closed geodesic in S of length at most 2π which determines a thin necklace or a short closed geodesic in S which determines a thick necklace consisting of short beads. By Lemmas 6.4, 6.5, and 6.6 there is a perturbation of γ that determines an annular gallery whose internal dual is a simple closed path P in the dual soccer tiling. Moreover, if c denotes the absolute value of the combinatorial turning angle for P , then $|P| + c \leq 14$ and the turn pattern for P does not contain three consecutive left turns or three consecutive right turns. Since P is embedded it divides the soccer tiling into two soccer diagrams D_1 and D_2 , one of which, say D_1 , has fewer than six pentagons. Since P , with the appropriate orientation is ∂D_1 , Theorem 3.10 implies that D_1 is one of the two soccer diagrams in Figure 2. Since both diagrams have $c = 4$ and $|\partial D| + c > 14$, we have a contradiction. \square

The final property that we need to establish is the following.

Lemma 6.8 (No flat planes). *If M is a closed 3-manifold with a metric $5/6^*$ -triangulation, then the universal cover \widetilde{M} does not contain any isometrically embedded flat planes.*

Proof. Let $\phi : \mathbb{R}^2 \rightarrow \widetilde{M}$ be an isometric embedding of a flat plane and let $F = \phi(\mathbb{R}^2)$. If F is transverse to an edge e in \widetilde{M} and x is the unique point in $e \cap F$, then the link of x in F is a closed geodesic loop γ of length 2π in the space of directions of x in \widetilde{M} . Since the space of directions of x is an orthogonal join of \mathbb{S}^0 with the metric circle which is the link of e in \widetilde{M} , the space of directions of x is either a standard 2-sphere (when the link of e has length exactly 2π) or a branched cover of \mathbb{S}^2 around antipodal points (when the link of e has length greater than 2π). Notice that in either case the loop γ must avoid the points corresponding to the edge e since F is transverse to e . In the branched case this is impossible and in the non-branched case, we can assume (Lemma 5.3) that e has degree 6 and is surrounded by six Coxeter tetrahedra. This shows that F cannot cross any edge of degree 5. Figure 14 shows an edge e of degree 6 surrounded by six Coxeter tetrahedra. Regardless of the location of the point x in e , there does not exist a portion of a flat plane through x which does not extend through one of the six edges

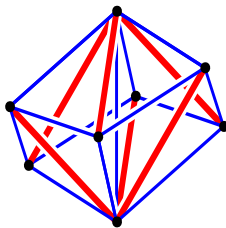


FIGURE 14. A cage around a degree 6 edge.

of degree 5. The key observation is that there are three edges of degree 5 extending down from the top of e , another three edges of degree 5 extending up from the bottom of e , and these six edges interleave. In other words, the edges of degree 5 form a cage from which a portion of a flat plane cannot escape.

The remaining possibility is that F is completely contained in the 2-skeleton of \widetilde{M} . If v is a vertex of \widetilde{M} contained in F , then the link of v in F corresponds to a closed geodesic loop of length 2π in the 1-skeleton of the link of v in \widetilde{M} . By Lemma 6.7 this is also impossible. \square

Theorem 1.2 (Main Theorem). *Every $5/6^*$ -triangulation of a closed 3-manifold M admits a piecewise Euclidean metric of non-positive curvature, where the universal cover \widetilde{M} contains no isometrically embedded flat planes. As a consequence, $\pi_1(M)$ is word-hyperbolic.*

Proof. Let M be such a piecewise Euclidean 3-manifold. By Theorem 4.1 it is sufficient to show that the links of the cells in M do not contain short geodesic loops. This is trivially true for the links of 3-cells and 2-cells (whose links are empty and discrete), and it is also true for links of 1-cells and 0-cells by Lemma 5.3 and Lemma 6.7. Thus M is non-positively curved. Since there are no isometrically embedded flat planes in \widetilde{M} by Lemma 6.8, the final assertion follows immediately from Theorem III.Γ.3.1 in [3]. \square

REFERENCES

- [1] B. H. Bowditch. Notes on locally $\text{cat}(1)$ spaces. In *Geometric group theory (Columbus, OH, 1992)*, pages 1–48. de Gruyter, Berlin, 1995.
- [2] Noel Brady, Jon McCammond, and John Meier. Bounding edge degrees in triangulated 3-manifolds. To appear in *Topology and its Applications*.
- [3] Martin R. Bridson and André Haefliger. *Metric spaces of non-positive curvature*. Springer-Verlag, Berlin, 1999.
- [4] D. Cooper and W. P. Thurston. Triangulating 3-manifolds using 5 vertex link types. *Topology*, 27(1):23–25, 1988.
- [5] Murray Elder and Jon McCammond. $\text{CAT}(0)$ is an algorithmic property. To appear in *Geometriae Dedicata*.
- [6] Murray Elder and Jon McCammond. Curvature testing in 3-dimensional metric polyhedral complexes. *Experimental Mathematics*, 11(1):143–158, 2002.

- [7] The GAP Group. *GAP – Groups, Algorithms, and Programming, Version 4.2*, 2000.
(\protect\vrule width0pt\protect\href{http://www.gap-system.org}{http://www.gap-system.org}).
- [8] Jonathan P. McCammond and Daniel T. Wise. Fans and ladders in small cancellation theory. *Proc. London Math. Soc. (3)*, 84(3):599–644, 2002.
- [9] John Sullivan. New tetrahedrally close-packed structures. Preprint 2000.

DEPT. OF MATHEMATICS, TUFTS UNIVERSITY, MEDFORD, MA 02155
E-mail address: `murray.elder@math.tamu.edu`

DEPT. OF MATHEMATICS, U. C. SANTA BARBARA, SANTA BARBARA, CA 93106
E-mail address: `jon.mccammond@math.ucsb.edu`

DEPT. OF MATHEMATICS, LAFAYETTE COLLEGE, EASTON, PA 18042
E-mail address: `meierj@lafayette.edu`